Journal of Catalysis 279 (2011) 196–204

Contents lists available at ScienceDirect

Journal of Catalysis

journal homepage: www.elsevier.com/locate/jcat

Cyanoethylation of alcohols by activated Mg–Al layered double hydroxides: Influence of rehydration conditions and Mg/Al molar ratio on Brönsted basicity

Jaime S. Valente [a,*], Heriberto Pfeiffer [b], Enrique Lima [b], Julia Prince [c], Jorge Flores [c]

[a] Instituto Mexicano del Petroleo, Eje Central 152, Mexico, D.F. 07730, Mexico
[b] Instituto de Investigaciones en Materiales, Universidad Nacional Autonoma de Mexico, Circuito Exterior s/n, Cd. Universitaria, Mexico, D.F. 04510, Mexico
[c] Universidad Autonoma Metropolitana-A, Av. San Pablo 180, Mexico, D.F. 02200, Mexico

ARTICLE INFO

Article history:
Received 20 December 2010
Revised 16 January 2011
Accepted 19 January 2011
Available online 22 February 2011

Keywords:
Cyanoethylation of alcohols
Layered double hydroxides
Meixnerite-like compounds
Basic catalysts
Brönsted basic sites

ABSTRACT

Activated Mg–Al layered double hydroxides (LDHs) with varying Mg/Al molar ratios are tested as heterogeneous catalysts for the cyanoethylation of methanol and 2-propanol. The activation procedure is performed by calcination of the LDH precursors, followed by gas-phase rehydration on an H_2O/N_2 flow. In this case, rehydration is carried out at 80 °C, instead of room temperature as usual. Increased temperature has a very significant effect on the reconstruction speed, shortening the process from ~12 to 0.5 h. Good conversions and yields to alkoxypropionitriles are obtained with thus activated LDHs. Correlations are established between basic strength, as determined by $CDCl_3$ adsorption followed by FTIR, and catalytic activity. Depending on alcohol acidity, greatest conversions are obtained over catalysts with Mg/Al molar ratios of 2 or 3. Solids are further characterized by X-ray diffraction, thermal gravimetric analyses, and ^{27}Al MAS NMR.

1. Introduction

Cyanoethylation reactions consist of the addition of compounds containing active hydrogen to the double bond of acrylonitrile. Alcohols react with acrylonitrile to give alkoxypropionitriles, which can be further converted to carboxylic acids or amines by hydrolysis or reduction, respectively. Industrially, important organic compounds and drug intermediates are obtained in this manner [1–3]. The reaction is base catalyzed, typically using homogeneous base catalysts such as alkali hydroxides [1] or anion-exchange resins [1]. Given that heterogeneous catalysts are environment friendly, easily handled and reusable, some efforts have been dedicated to studying basic solids suitable for this reaction [2–5]. Various solids have been tested, including alkaline earth oxides and hydroxides [2], as well as activated [3] and/or rare-earth-modified [4,5] layered double hydroxides (LDHs).

LDHs are a family of anionic clays that have received much attention in the past decades, due to their vast applicability in diverse fields [6–8]. The LDH structure resembles that of brucite, where $M^{2+}(OH)_6$ octahedra share edges to build infinite $M(OH)_2$ sheets. An LDH is created by partial isomorphic substitution of divalent cations for trivalent ones, such that the layer acquires a positive charge. This charge is electrically balanced by anionic species located in the interlayer region, along with hydration water molecules. LDHs are represented by the general formula $[M^{2+}_{(1-x)}M^{3+}_x(OH)_2]A^{n-}_{x/n} \cdot mH_2O$, where M^{2+} and M^{3+} are metal cations capable of occupying the octahedral interstices of a brucite-like sheet, *i.e.* mainly those from the third and fourth periods, while A^{n-} may be virtually any organic or inorganic anion [6–8].

LDHs are also known as hydrotalcite-like compounds by reference to the naturally occurring Mg–Al–CO_3 hydrotalcite mineral. Upon calcination, it progressively suffers the loss of physisorbed and interlayer water, decomposition of interlayer anions and dehydroxylation of brucite-like sheets. Above ~300 °C, the layered structure collapses, and at approximately 400 °C, the solid crystallizes in MgO rock-salt like structure, with Al^{3+} cations evenly distributed, i.e. Mg(Al)O. It presents relatively large specific surface areas (>200 $m^2\,g^{-1}$) and strong Lewis basic sites, O^{2-} species. Therefore, it has found application as basic catalyst in numerous chemical reactions [9,10].

Most of the calcination products from the LDH family, including the Mg(Al)O mixed oxide, have the remarkable capacity of recovering their original layered structure when contacted with anions and/or water at low temperatures. This property is known as memory effect [6], and it has been exploited for incorporating interlayer anions different from the original ones, such as anionic contaminants [11]. When the calcined MgAl LDH is exposed to water or water vapor, the LDH structure is recovered, incorporating OH^- as charge-balancing anions, provided that care is taken to avoid CO_2 contamination [12]. The Mg–Al–OH LDH is commonly known as meixnerite, meixnerite-like, or activated LDH. The OH^- groups

* Corresponding author.
E-mail addresses: jsanchez@imp.mx, sanchezvalente@yahoo.com (J.S. Valente).

0021-9517/$ - see front matter © 2011 Elsevier Inc. All rights reserved.
doi:10.1016/j.jcat.2011.01.018

are capable of acting as Brönsted basic sites in catalytic reactions [12,13]. Activated LDHs have shown high catalytic activity in several reactions of industrial interest, such as aldol condensation [12,14], Claisen–Schmidt condensation [15], Knoevenagel reaction [16], and cyanoethylation of alcohols [3,4,17].

Given its importance, many efforts have been dedicated to understanding the calcination–reconstruction process of LDHs [14,18–30]. It is generally accepted that microstructural changes take place, i.e. the process is not entirely reversible. However, the precise nature and extent of these changes, the influence of the reconstruction procedure and conditions on the structure, and their combined effect on catalytic activity are not fully understood yet. Neverthless, it is accepted that the properties and catalytic activity of meixnerite depend to a large extent on the experimental procedure and conditions [14,24,25]. Usually, rehydration is carried out using a water-saturated N_2 flow, at room temperature and for varying time periods. Alternatively, mexinerite-like compounds may be prepared by liquid-phase reconstruction of the calcined LDH or by direct anion-exchange of an as-synthesized LDH.

In this sense, it was recently reported that varying the relative humidity and especially the temperature of the H_2O/N_2 flow has a significant effect on reconstruction speed and on the activation energy of the process [31]. Reconstruction was observed to proceed faster to completion at higher temperatures. It is to be expected, then, that shorter rehydration times will be required to reach the greatest catalytic activity when reconstruction is carried out at higher temperatures. Furthermore, reconstruction speed was found to be highly dependent on the Mg/Al molar ratio [32].

Moreover, even though high catalytic activities are obtained over activated LDHs in many industrially relevant reactions, and despite the clear advantages of a heterogeneous catalytic system, the industrial application of activated LDHs is not yet as widespread as one may expect. This is due to several obstacles, such as the rapid deactivation upon ambient CO_2 exposure, the difficulty in synthesizing LDHs on a large scale, and the lengthy catalyst reactivation procedure [33]. Efforts must be made to surmount these obstacles. Accordingly, in cyanoethylation reactions, activated LDHs have been observed to remain active after prolonged contact with air [3], which would greatly facilitate handling during industrial operation. Furthermore, an environment friendly, easily scalable method for LDH synthesis has been developed and was presented recently [34–36]. Additionally, in this work, it is demonstrated that the catalyst (re)activation time may be considerably shortened by performing rehydration at 80 °C instead of room temperature. Hence, this may bring us one step closer to the industrial application of activated LDHs.

Thus, this paper focuses on studying the cyanoethylation of two alcohols, methanol and 2-propanol, using meixnerite-like catalysts with different Mg/Al molar ratios. Rehydration of calcined LDHs was performed at 80 °C, for varying time periods (0.5–3 h), to investigate the effect of rehydration conditions on catalytic activity. A correlation is established between catalytic activities and the strength of basic sites.

2. Experimental

2.1. Catalyst synthesis and activation

MgAl LDHs with varying Mg/Al molar ratios were prepared by the coprecipitation at low supersaturation method. An aqueous solution (1 M) was prepared by dissolving the appropriate amounts of $Mg(NO_3)_2{\cdot}6H_2O$ and $Al(NO_3)_3{\cdot}9H_2O$ in distilled water. Separately, a 2 M alkaline solution containing K_2CO_3 and KOH was prepared. Both solutions were added simultaneously to a glass reactor, maintaining the pH constant at 9.0. The precipitate was kept under vigorous stirring at 80 °C for 18 h. Then, it was washed repeatedly with hot deionized water and dried at 100 °C for 24 h. As-synthesized samples were labeled *X*MgAl, where *X* stands for the Mg/Al molar ratio.

The catalyst activation was performed in a two-step process. Typically, 0.2 g of the as-synthesized MgAl LDH was heat-treated in flowing N_2 (100 mL min^{-1}), with a heating rate of 10° min^{-1}, up to 500 °C, where it was maintained for 5 h. Afterward, the sample was cooled down to 80 °C, and the rehydration process was carried out using an N_2 flow (60 mL min^{-1}) saturated with water, for 0.5, 1, or 3 h. The deionized, decarbonated water contained in the saturator was heated at 80 °C in order to maintain water partial pressure constant at 47.4 kPa in the N_2/water vapor mixture. All in and out stainless steel lines were heated in order to avoid water condensation. Once the established rehydration time concluded, the reconstructed LDH was flushed with a pure N_2 stream (100 mL min^{-1}) for 0.5 h in order to eliminate excess water. Finally, the solid was allowed to cool down to room temperature. Activated catalysts were labeled *X*MgAl-R*Y*, where *X* stands for the Mg/Al molar ratio and *Y* the rehydration time, in hours (0.5, 1 or 3 h).

2.2. Characterization techniques

The chemical composition of solids was determined in a Perkin-Elmer model Optima 3200 Dual Vision by inductively coupled plasma atomic emission spectrometry (ICP-AES).

X-ray diffraction patterns were recorded using $CuK_{\alpha 1}$ radiation (λ = 1.54 Å) on a Philips X'Pert instrument operating at 45 kV and 40 mA in the 2θ range of 4–80°, with a step size of 0.02° and step scan of 0.4 s.

Thermogravimetric (TG) analyses were carried out on a Netzch STA-409EP equipment which was operated under a nitrogen flow, at a heating rate of 10 °C min^{-1} from 25 to 1000 °C. In all determinations, 100 mg of finely powdered dried LDH sample was used.

The single pulse solid-state ^{27}Al MAS NMR spectra were acquired under MAS conditions on a Bruker Avance 300 spectrometer, at 7.05 Tesla. A short pulse ($\pi/12$) width of 1 μs was employed to ensure quantitative reliability of the intensities observed for the ^{27}Al central transition for sites experiencing different quadrupole couplings. Spinning speed of samples was 10 kHz, and at least 5000 scans were performed. Chemical shifts are expressed as ppm of aqueous complex $[Al(H_2O)_6]^{3+}$.

Deuterated chloroform was used as a basicity probe molecule, followed by diffuse reflectance infrared Fourier-transform spectroscopy (DRIFTS), which was carried out in a Bruker Equinox 55 spectrometer, between 4000 and 400 cm^{-1} with a resolution of 4 cm^{-1} after 600 scans per spectrum. The equipment was furnished with a Harrick Praying Mantis chamber allowing *in situ* treatments up to 450 °C. Activated catalysts were rapidly transferred into the chamber, which was previously purged with a He flow to ensure an inert atmosphere. The samples were allowed 5 min in a He flow (5 mL min^{-1}), and then the chamber was sealed. Spectra were recorded at room temperature and static helium atmosphere, prior to and immediately following injection of 2 μL of $CDCl_3$. Then, He flow was restarted, and the sample was heated up to 450 °C, recording spectra at 50° intervals, allowing 1 h stabilization at each temperature.

2.3. Cyanoethylation catalytic tests

The cyanoethylation reaction procedure was similar to that previously reported [3]. Typically, 80 mmol of acrylonitrile and 20 mL of alcohol (methanol or 2-propanol) were added to a three-necked 50-mL round-bottom flask equipped with a reflux condenser and a thermometer. The solution was magnetically stirred at 50 °C, and the freshly activated catalyst was rapidly added to the reactor in

order to minimize exposure to atmospheric CO_2. Once the reaction started, aliquots were periodically taken from the reaction mixture, filtered and analyzed on an HP-6890 GC equipped with a 60-m HP-5 (5%-phenyl-methylpolysiloxane) capillary column. Conversion was calculated following the decrease in acrylonitrile concentration.

3. Results and discussion

3.1. Catalyst characterization

3.1.1. As-synthesized LDHs

The chemical composition of the solids and their Mg/Al molar ratios, displayed in Table 1, are close to the nominal values, within experimental error.

X-ray diffraction patterns of as-synthesized LDHs, presented in Fig. 1, reveal a pure LDH phase. XRD patterns are characterized by strong, sharp peaks at low 2θ values, belonging to basal spacing 0 0 l reflections, and smaller in-plane diffraction peaks at high angles. Cell parameters c and a of the triple hexagonal unit cell, calculated assuming a $3R_1$ polytype, are presented in Table 1.The $c = 3d_{003}$ parameter is indicative of interlayer distance, and the $a = 2d_{110}$ parameter is related to the average cation–cation distance in the brucite-like sheets.

Both unit cell parameters clearly increase along with the Mg/Al molar ratio. The increase in interlayer distance is due to the decrement in layer charge density. With lower Mg/Al molar ratio, i.e. larger Al^{3+} substitution degree x, there is a stronger electrostatic attraction between positively charged sheets and interlayer anions. Therefore, the layers are packed closer together in LDHs with lower Mg/Al ratio. Furthermore, interlayer distances are well in agreement with CO_3^{2-} intercalated LDHs in all cases.

Correspondingly, the a cell parameter is known to obey Vegard's law for solid solutions. The average cation–cation distance decreases with the isomorphous substitution of Mg^{2+} by Al^{3+} (lower Mg/Al molar ratio), given that their Shannon octahedral coordination ionic radii are 0.72 Å and 0.535 Å, respectively [37]. Therefore, the observed increase in a values corroborates the intended variation of Mg/Al molar ratios. Additionally, a values agree well with those reported for MgAl samples with similar chemical compositions [38], confirming the complete incorporation of the metal cations to the brucite-like sheets.

3.1.2. Thermal decomposition of as-synthesized LDHs

The thermal decomposition process of MgAl–CO_3 LDHs is well documented [6–8,39]. Initially, between room temperature and 250 °C, physisorbed water molecules are lost, followed by interlayer water molecules, possibly along with small amounts of weakly bound OH groups and physisorbed CO_2. From 250 °C and up to 450 °C, CO_2 is evolved from interlayer carbonate, and water and OHs from the dehydroxylation of the brucite-like sheets.

Table 1
Unit cell parameters and chemical compositions of as-synthesized MgAl LDHs with varying molar ratios.

Sample	Unit cell parameters (Å)		General formula	Mg/Al molar ratio
	c	a		
2MgAl	22.804	3.046	$[Mg_{0.675}Al_{0.324}(OH)_2](CO_3)_{0.162} \cdot 0.77H_2O$	2.08
2.5MgAl	23.173	3.054	$[Mg_{0.733}Al_{0.267}(OH)_2](CO_3)_{0.133} \cdot 0.80H_2O$	2.75
3MgAl	23.367	3.059	$[Mg_{0.745}Al_{0.255}(OH)_2](CO_3)_{0.127} \cdot 0.80H_2O$	2.93
3.5MgAl	23.707	3.070	$[Mg_{0.773}Al_{0.227}(OH)_2](CO_3)_{0.114} \cdot 0.98H_2O$	3.40
4MgAl	23.802	3.072	$[Mg_{0.790}Al_{0.210}(OH)_2](CO_3)_{0.105} \cdot 1.05H_2O$	3.78

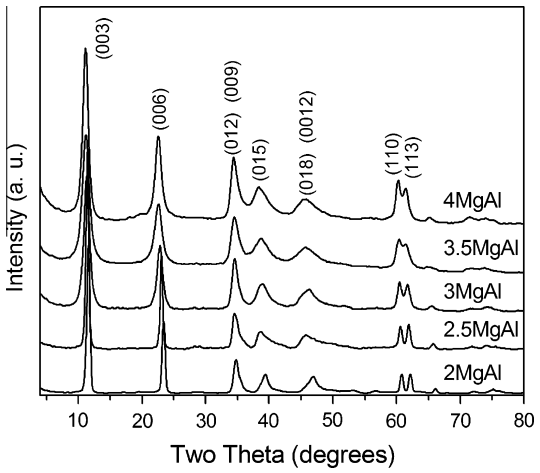

Fig. 1. X-ray diffraction patterns of as-synthesized LDHs.

Weight percentage losses, as measured by TGA, correspond to approximately 19 and 22 wt.% for the first and second stages, respectively.

Only small deviations in weight percentage losses with varying Mg/Al molar ratios were detected on the TGA profiles (data not shown). The samples with a higher Mg/Al molar ratio, 3.5MgAl and 4MgAl, contain larger amounts of hydration water molecules, evidenced by a greater weight loss in the first thermal event (25–250 °C). This phenomenon could be attributed to the lower amount of interlayer anions present in samples with greater Mg/Al molar ratio, which leaves more room for the intercalation of water molecules. Contrarily, the amount of weight lost during the second thermal event increases with decreasing Mg/Al ratio, due to the larger amount of interlayer anions.

Furthermore, as may be observed in DTG profiles in Fig. 2, the temperature at which the first thermal event occurs is dependent on the Mg/Al ratio. This peak becomes broader and shifts to lower temperatures with increasing molar ratio, due to the larger amount of water, in agreement with previously discussed TGA profiles. Moreover, it is worth noting that the interlayer region of LDHs is made up of an intricate system of hydrogen bonds, between layer OH groups, interlayer anions, and water molecules [8]. Then, the shift to lower temperatures could be due to the lower layer charge density and fewer interlayer anions, as this would reduce the strength of the hydrogen bonding network and facilitate water departure. Also, the larger interlayer distance in samples with higher Mg/Al molar ratio (Table 1) implies less diffusional barriers for departing molecules. On the other hand, the temperature of the second thermal event, at which interlayer anions are lost, shows no clear dependence on the Mg/Al molar ratio.

3.1.3. Activated LDHs

3.1.3.1. Structural analyses. It is well known that upon calcination, the layered structure collapses and the solid then crystallizes in MgO rock-salt like structure [6–8,30]. Accordingly, XRD patterns of calcined samples revealed pure MgO phase (data not shown). When the calcined samples are placed in a decarbonated water-saturated N_2 flow, they recover their original layered structure, incorporating OH^- groups as charge-balancing anions. The obtained Mg–Al–OH LDH is commonly known as activated LDH, meixnerite, or meixnerite-like. The reconstruction process is traditionally carried out at room temperature and lasts an average of 12 h. However, it was recently reported that process conditions, such as relative humidity and temperature, have a major influence in the process' activation energies and the overall reconstruction speed [31,32].

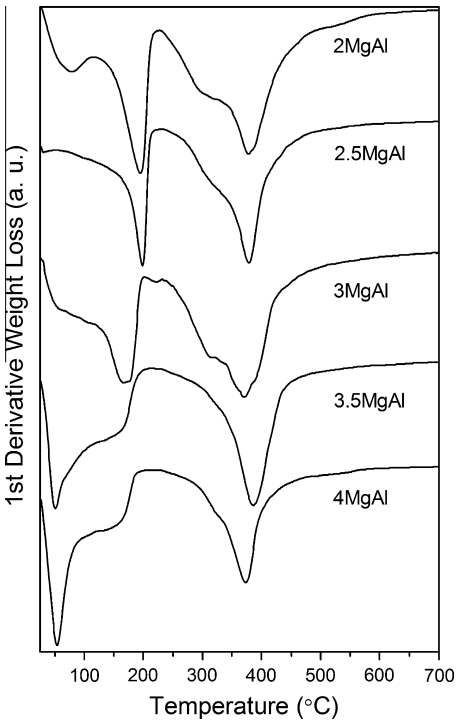

Fig. 2. Differential thermal gravimetric profiles of indicated samples.

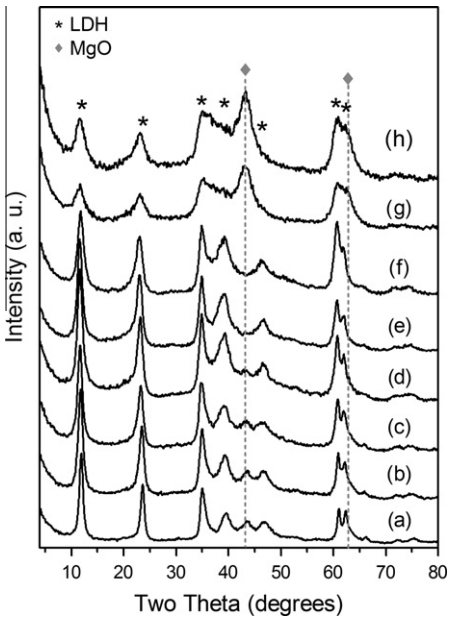

Fig. 3. X-ray diffraction patterns of activated LDH catalysts: (a) 2MgAl-R0.5, (b) 2MgAl-R1, (c) 2.5MgAl-R0.5, (d) 3MgAl-R0.5, (e) 3MgAl-R1, (f) 3.5MgAl-R0.5, (g) 4MgAl-R0.5, (h) 4MgAl-R1.

In this case, samples were activated at 100% relative humidity and 80 °C, for 0.5, 1, or 3 h. In a very short time, only 0.5 h, the layered structure is almost entirely recovered, as may be appreciated in the XRD patterns of Fig. 3. The reconstruction rate is dependent on the Mg/Al molar ratio, in agreement with a previous report [32]. Sample 4MgAl-R0.5 shows the slowest reconstruction rate. Its most prominent diffraction peak, located at ~43° 2θ, belongs to MgO. Also, it is interesting to notice that for a given chemical composition, there are no major changes in XRD patterns when the rehydration time is increased from 0.5 to 1 h (Fig. 3).

Cell parameters of reconstructed samples are presented in Table 2. The *c* cell parameter is slightly decreased, compared to the as-synthesized samples. Interlayer distances coincide with those reported for OH^- intercalated LDHs [6]. The low *c* value is related to the similarity of OH^- and H_2O ionic diameters, and to the strong hydrogen bridges among water and OH^-, leading to the best close-packed arrangement [6].

Furthermore, comparing the *a* cell parameter of as-synthesized and reconstructed LDHs with a given molar ratio, one notices a small decrease in all cases. As mentioned previously, the *a* parameter is related to the Mg/Al molar ratio in the brucite-like sheets. Then, this decrease is associated with a higher relative amount of aluminum in the layers. It may be interpreted as an incomplete incorporation of Mg^{2+} to the LDH phase. Accordingly, an MgO phase is observed in most of these samples' XRD patterns and is probably still present even when MgO is no longer detected by XRD. However, it is interesting to remark that apparently, Al^{3+} returns to the LDH phase faster than Mg^{2+}. Moreover, comparing sets of samples with the same chemical composition and different rehydration times (e.g. 2MgAl-R0.5 and 2MgAl-R1), it is clear that Mg^{2+} continues to incorporate itself to the brucite-like layers, given the increase in *a* parameter values (Table 2).

3.1.3.2. ^{27}Al MAS NMR. Typically, an as-synthesized MgAl LDH presents only aluminum species in octahedral coordination (Al^{VI}). In the course of thermal treatment, a fraction (approximately 20%) of Al species is expected to migrate to tetrahedral sites (Al^{IV}). Then, during reconstruction, if sufficient time is given, all Al atoms recover their initial octahedral coordination [14]. Therefore, the reconstruction degree may also be estimated by means of ^{27}Al MAS NMR spectroscopy. The spectra presented in Fig. 4 show a very intense NMR signal close to 0 ppm, indicating Al species in octahedral coordination (Al^{VI}) on brucite-like layers. A second, smaller resonance signal close to 70 ppm is also appreciated, denoting a small fraction of Al in tetrahedral coordination (Al^{IV}). All MgAl LDHs present Al^{IV}, after 0.5 and 1 h reconstruction, indicating that the LDH structure has not been fully recovered. The relative percentages of Al^{IV} and Al^{VI} are presented in Table 2.

The amount of tetrahedral aluminum decreases when the rehydration time is increased from 0.5 to 1 h, for a given chemical composition. In addition, if samples with the same rehydration time are compared (0.5 h), a clear dependency on Mg/Al molar ratio is observed. The rapidity with which aluminum regains octahedral coordination is 3MgAl-R0.5 > 3.5MgAl-R0.5 > 2MgAl-R0.5 ≈ 2.5MgAl-R0.5 ≫ 4MgAl-R0.5.

Total reconstruction of the layered structure may not be required for catalytic purposes. Indeed, the most favorable reconstruction time varies from one catalytic reaction to the other. This may be related to the strength of the basic sites created at different rehydration stages.

3.1.3.3. Basicity measurements. The quantification of the basic strength of Brönsted sites in reconstructed LDHs may be performed by adsorption of suitable probe molecules followed by FTIR spectroscopy [40,41]. Deuterated chloroform may be used as IR probe of basic surface sites, since it is a weak acid that should not suffer important chemical transformations at the tested conditions, other than the acid–base associative interactions [42,43]. It is a relatively small molecule capable of accessing the basic sites that may participate in the cyanoethylation reaction. The main ν_{CD} stretching vibration band, which appears at 2264 cm^{-1} on the gas phase, does not overlap the bands of surface OH groups, enabling straightforward identification. $CDCl_3$ has the ability of establishing hydrogen bond interactions with basic sites, which are manifested by a

Table 2
Unit cell parameters, relative populations of tetrahedral (Al^{IV}) and octahedral (Al^{VI}) aluminum species from deconvoluted ^{27}Al MAS NMR spectra, and estimated p*K*a values of indicated catalysts.

Sample	Unit cell parameters (Å)		Relative population (%)		Estimated p*K*a of basic sites[a]
	c	*a*	Al^{IV}	Al^{VI}	
2MgAl-R0.5	22.278	3.035	9	91	–
2MgAl-R1	22.528	3.042	4	96	+14.6
2.5MgAl-R0.5	22.751	3.049	9	91	+15.3, +19.2
3MgAl-R0.5	22.703	3.047	5	95	+15.5, +19.5
3MgAl-R1	22.788	3.052	4	96	+10.6, +15.5, +19.5
3.5MgAl-R0.5	22.534	3.052	6	94	+11.6
4MgAl-R0.5	22.703	3.051	17	83	–
4MgAl-R1	22.541	3.053	13	87	–

[a] Estimated by the $\Delta\nu$ of the C–D vibration band of adsorbed $CDCl_3$ [42,43].

red-shifting of the ν_{CD} band. The magnitude of the shift is related to the basic strength; a correlation between $\Delta\nu_{CD}$ and the p*K*a values of the basic centers was established by Paukshtis et al. [42,43].

Representative spectra for sample 2.5MgAl-R0.5 in the ν_{CD} region are shown in Fig. 5. A reference spectrum was first recorded and then the spectrum after adsorption of 2 μL $CDCl_3$. As may be observed, upon $CDCl_3$ adsorption, there are two appreciable differences in the spectra. On one hand, there appears a small, broad, two-component band with maxima at 2173 and 2119 cm^{-1}, which is ascribed to the ν_{CD} stretching band. As expected, the band has shifted to lower frequencies due to hydrogen bond interactions with basic sites. The two maxima must then correspond to basic sites of different strength. According to the correlations established by Paukshtis et al., $\Delta\nu_{CD}$ of 91 and 145 cm^{-1} correspond to proton affinities of *ca.* 965 and 1000 kJ mol^{-1}, and the estimated p*K*a values are +15 and +19, respectively [42,43].

The other spectral modification is seen in the OH region. Specifically, a shoulder appears between ~2600 and 2400 cm^{-1}. This band is ascribed to an O–D stretching vibration. In solid HDO, where all molecules are tetrahedrally hydrogen-bonded, the O–D

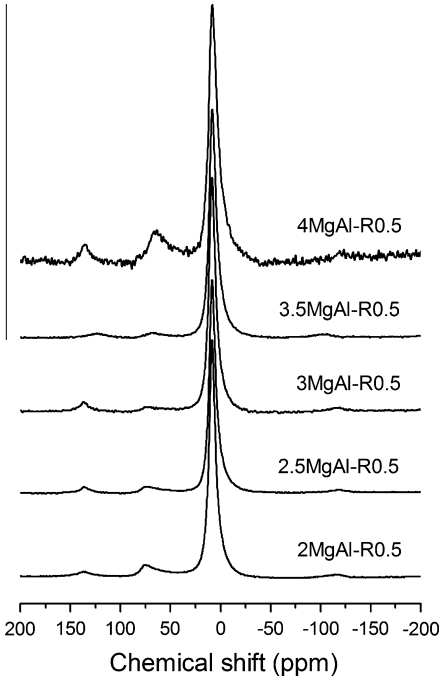

Fig. 4. ^{27}Al MAS NMR spectra of indicated catalysts.

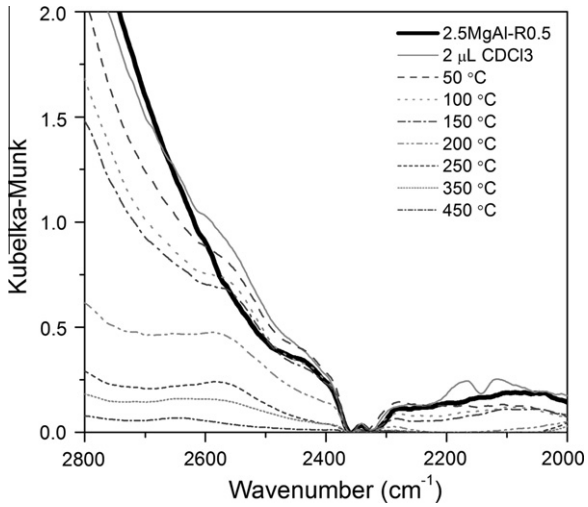

Fig. 5. FTIR spectra of catalyst 2.5MgAl-R0.5, taken prior (—) and subsequent (—) to $CDCl_3$ adsorption, and then at indicated temperatures during thermal decomposition of $CDCl_3$-adsorbed 2.5MgAl-R0.5.

vibrational frequency is 2416 cm^{-1} [44]. In this case, because of increased relaxation of the molecule, the band is blue-shifted, approximately 100 cm^{-1}. The appearance of an O–D vibration implies that a proton-exchange reaction, between an OH^- basic site and deuterium, has taken place. This provides further evidence of the strong interaction that occurs between chloroform and the Brönsted sites. A similar phenomenon was observed previously with LDH-derived MgGa mixed oxides with similar basic strengths [45].

Once the adsorption spectrum was recorded, the sample was set in a He flow (5 mL min^{-1}) and heat-treated *in situ,* to investigate thermal behavior. As soon as the He flow was started, the ν_{CD} vibration bands close to 2200 cm^{-1} disappeared, in agreement with previous observations [24,45].

In LDHs, the broad OH vibration band in the 3800–2400 cm^{-1} region is in fact the result of two or even three overlapping OH stretching vibrations, plus a vibration due to interlayer water [7]. Upon heating, physisorbed water molecules, interlayer water, hydroxyls from brucite-like layers, and charge-compensating OH^- groups are progressively lost. Remarkably, the O–D vibration, centered at ~2550 cm^{-1}, persists at temperatures as high as 250 °C. Therefore, it is reasonable to assume that the proton-exchange reaction took place with interlayer OH^- anions, which are lost approximately at this temperature. These anions are likely the strongest Brönsted basic sites of the catalyst.

The interactions between the catalysts and $CDCl_3$ may be straightforwardly observed by subtracting the spectra acquired prior and subsequent to $CDCl_3$ adsorption. Fig. 6 presents differential spectra of $CDCl_3$ adsorbed on several catalysts. Also, the p*K*a values of the Brönsted basic sites, estimated by the magnitude of the red shift of the ν_{CD} stretching band [42,43], are summarized in Table 2. Spectra of all analyzed catalysts, in the ν_{CD} region, may be found in the Supplementary data.

The previously discussed observations regarding $CDCl_3$ adsorption on sample 2.5MgAl-R0.5 are unmistakably observed in the differential spectrum, i.e. the ν_{OD} stretching vibration at 2551 cm^{-1} and the shifted ν_{CD} bands at 2173 and 2119 cm^{-1} (Fig. 6). The other catalysts present somewhat similar behaviors. In 2MgAl-R0.5, there is a single, strong, narrow band in the differential spectra, centered at 2530 cm^{-1}, assigned to the stretching O–D vibration. No other bands that could be attributed to a shifted ν_{CD} band are detected. This may be understood as a very strong interaction of $CDCl_3$ with the basic sites of this sample, so that they completely

undergo proton-exchange reactions. Thus, it is inferred that 2MgAl-R0.5 has the strongest Brönsted basic sites of the analyzed catalysts. It is worth mentioning that the thermal behavior of this O–D band is very similar to that previously described for 2.5MgAl-R0.5 (see Supplementary data).

In sample 3MgAl-R0.5, two peaks at 2171 and 2114 cm^{-1}, assigned to the shifted ν_{CD} band, are appreciated. These bands also correspond to basic sites with approximate p*K*a values of +15 and +19 (Table 2). There is also a weak band around 2534 cm^{-1}, which is ascribed to a proton-exchange reaction that occurs only to a very limited extent. This may indicate that sample 3MgAl-R0.5 has fewer strong basic sites than the catalysts with lower Mg/Al molar ratio or that these sites are less accessible to $CDCl_3$.

For sample 3.5MgAl-R0.5, the interaction with $CDCl_3$ was very weak. A very small band, attributed to the ν_{CD} vibration, appeared at 2205 cm^{-1}. Based on the magnitude of $\Delta\nu$, the estimated p*K*a of these basic sites is +11.6. Samples 4MgAl-R0.5 and 4MgAl-R1, apparently have no interaction with $CDCl_3$ (see Supplementary data), as no spectral differences were detected before and after $CDCl_3$ adsorption. This may be attributed to a lower basicity of these samples. Accordingly, it has been reported that higher Mg/Al molar ratios induce higher acidity and lower basicity in both calcined [46] and activated [13] MgAl LDHs. In activated LDHs, samples with larger Mg/Al molar ratio (lower layer charge density) have fewer charge-balancing OH^- anions and therefore less Brönsted basic sites. Furthermore, bonding between octahedral layers and interlayers involves a combination of electrostatic effects and hydrogen bonding. Hydroxyl groups bonded to trivalent cations are strongly polarized and interact with interlayer anions [8]. Thus, layer OH groups in solids with lower layer charge density are less polarized, and the negative charge density carried by interlayer anions is also lowered. Then, the basic strength of the interlayer OH^- Brönsted sites is decreased when the Mg/Al ratio rises.

The effect of increasing rehydration time on basic strength is observed when the differential spectra of samples 2MgAl-R0.5 and 2MgAl-R1 are compared (Fig. 6). In the latter, the ν_{OD} band is broader, and a small peak is detected at 2178 cm^{-1}, which corresponds to basic sites with p*K*a of approximately +15. For catalyst 3MgAl, when rehydration time was increased to 1 h, a small band appeared at 2213 cm^{-1}. The bands at 2171 and 2114 cm^{-1} observed on 3MgAl-R0.5 are still present, albeit with reduced intensity (Supplementary data). The 2213 cm^{-1} band is ascribed to newly created, weaker Brönsted basic sites, with estimated p*K*a value of +10.6. Hence, it may be concluded that prolonging rehydration time could engender new, weaker basic sites. The sites that are first hydrated are the most reactive and thus the ones with strongest basicity. Increasing water amounts will progressively generate more basic sites, until all available sites are hydrated. From this point on, further rehydration will very likely poison basic sites.

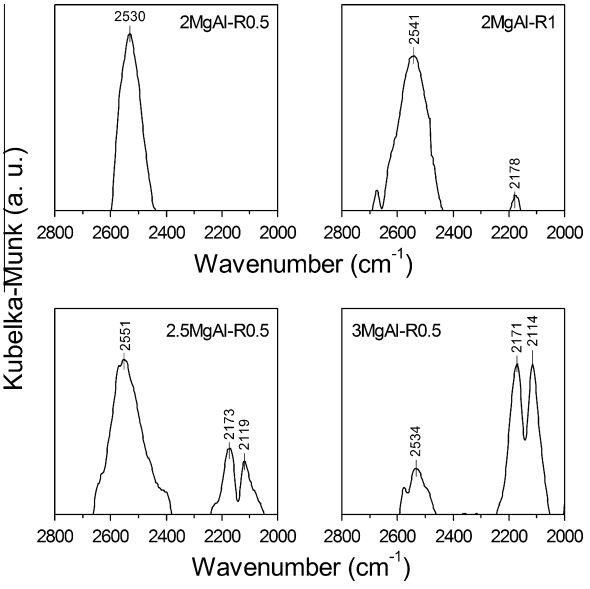

Fig. 6. Differential FTIR spectra of $CDCl_3$ adsorbed on indicated catalysts.

3.2. Cyanoethylation of methanol and 2-propanol

3.2.1. Reaction mechanism

The cyanoethylation of alcohols reaction is thought to proceed in a 3-step process. The mechanism presented in Scheme 1 was derived for a homogeneous system and adapted by analogy to heterogeneous catalysts [2]. In step 1, the Brönsted basic site abstracts a proton from the hydroxyl group of the alcohol, producing an adsorbed alkoxide anion. This anion is stabilized on a surface acid site. Given that both Brönsted and Lewis acid sites are present in these catalysts, the acidic site is depicted by A. Afterward, in step 2, the adsorbed alkoxide anion reacts with the double bond of acrylonitrile to form an adsorbed 3-alkoxypropanenitrile anion. This anion takes an H^+ from the basic site in step 3, to yield 3-alkoxypropanenitrile and conclude the catalytic cycle.

Both step 1 and step 2 may be the rate-limiting reaction steps. If the catalysts have relatively weak basic sites, the slowest step will be the proton abstraction in step 1. In this case, reaction rate is determined by the acidity of the alcohol, which determines the ease of abstraction of H^+. On the other hand, on catalysts with strong basic sites, proton abstraction should not represent an obstacle. Reaction rate would then be determined by the stability of the alkoxide anion in step 2.

3.2.2. Influence of Mg/Al molar ratio

Cyanoethylation of methanol and 2-propanol was carried out to determine the catalytic activity of the activated LDHs with varying Mg/Al molar ratios. Selectivities of 100% to the corresponding alkoxypropionitrile were obtained with both alcohols in all cases. Initial reaction rates, as well as yields to the corresponding alkoxypropionitrile, are presented in Table 3.

Fig. 7 presents results from the cyanoethylation of methanol by several activated LDHs, all with 0.5 h reconstruction time. As may be observed, the highest activity was displayed by catalyst 3MgAl-R0.5, closely followed by 2.5MgAl-R0.5, then 2MgAl-R0.5. Catalyst 3.5MgAl-R0.5 presents considerably less activity, while 4MgAl-R0.5 was inactive (not shown). According to the reaction mechanism, for methanol, being the most acidic aliphatic alcohol, proton abstraction is most likely not an obstacle. Step 2, related to the stability of the methoxide anion (Scheme 1), should be the rate-limiting step. Catalytic activity decreases as 3MgAl-R0.5 > 2.5MgAl-R0.5 > 2MgAl-R0.5. Thus, among the strongest basic catalysts, methoxide reactivity is inversely proportional to basic strength, as determined by $CDCl_3$ adsorption (Section 3.1.3.3). Initial reaction rates are 26, 23, 13, and 2×10^{-3} mol g^{-1} min^{-1} for 3MgAl-R0.5, 2.5MgAl-R0.5, 2MgAl-R0.5, and 3.5MgAl-R0.5, respectively (Table 3). It is further interesting to notice that conversions continue to increase with reaction time, particularly on the least active catalysts. At 60 min reaction, yields are above 90% for the three most active catalysts (Table 3); meanwhile, 3.5MgAl-R0.5 attains 92% conversion at 85 min (Fig. 7).

On the other hand, when these catalysts were tested for the cyanoethylation of 2-propanol, a nearly inverse activity trend was observed (Fig. 8). The most active catalyst was 2MgAl-R0.5, followed by 2.5MgAl-R0.5, then 3MgAl-R0.5, 3.5MgAl-R0.5, and 4MgAl-R0.5. The observed trend is well in agreement with the basic strength determined by $CDCl_3$ adsorption (Section 3.1.3.3) and

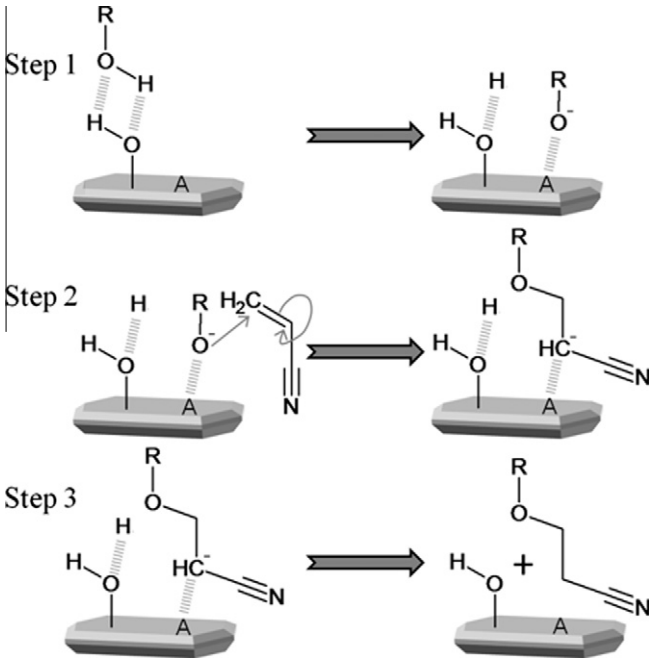

Scheme 1. Proposed reaction mechanism for the cyanoethylation of alcohols over rehydrated MgAl LDHs.

with the reaction mechanism (Section 3.2.1) discussed previously. In the case of 2-propanol, the rate-limiting step likely is proton abstraction in Step 1 (Scheme 1), since it is a weaker acid than methanol. Then, stronger basic sites are required, and the reaction proceeds faster on 2MgAl-R0.5 and decreases with decreasing basic strength and decreasing Mg/Al molar ratio.

It is worth noting that 3.5MgAl-R0.5 and 4MgAl-R0.5 are the least active catalysts in the cyanoethylation of both alcohols. This is in agreement with observations from $CDCl_3$ adsorption followed by FTIR, which indicate that samples with highest Mg/Al molar ratio have the weakest basic sites. Furthermore, these solids require less charge-balancing anions and therefore have fewer Brönsted basic sites. In all cases, greater conversions were obtained with methanol than with 2-propanol, with the exception of 4MgAl-R0.5, which is almost not reactive in either case.

3.2.3. Influence of rehydration time

The effect of rehydration time was evaluated on several catalysts. Cyanoethylation of methanol was carried out over catalyst

Table 3
Initial reaction rates and yields obtained for the cyanoethylation of methanol and 2-propanol over indicated catalysts.

Catalyst	Initial reaction rate (mol g^{-1} min^{-1} × 10^3)		Yield to alkoxypropionitrile[a] (%)	
	Methanol	2-Propanol	Methanol	2-Propanol
2MgAl-R0.5	13	12	91	65
2MgAl-R1	n.d.	13	n.d.	69
2MgAl-R3	n.d.	8	n.d.	50
2.5MgAl-R0.5	23	6	100	58
3MgAl-R0.5	26	6	97	48
3MgAl-R1	33	7	100	63
3MgAl-R3	24	n.d.	100	n.d.
3.5MgAl-R0.5	2	2	75	41
3.5MgAl-R3	7	n.d.	95	n.d.
4MgAl-R0.5	0	2	0	5
4MgAl-R3	0	n.d.	5	n.d.

[a] Calculated at 60 min reaction time.

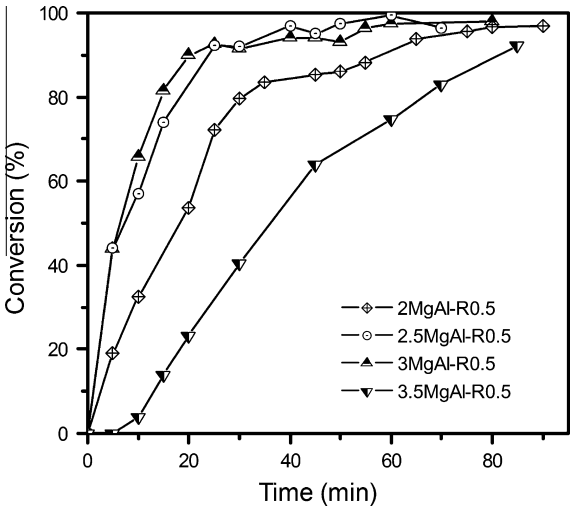

Fig. 7. Cyanoethylation of methanol over catalysts with varying Mg/Al molar ratios and 0.5 h rehydration time.

3MgAl, rehydrated for different times: 0.5, 1, and 3 h. It was observed that increasing rehydration time from 0.5 to 1 h had a minor beneficial effect on catalytic activity. Meanwhile, if the rehydration step is prolonged for 3 h, there is a somewhat detrimental effect on the initial reaction rate. In all cases, conversions above 95% are reached in less than 1 h (Fig. 9); nonetheless, initial reaction rates are 26, 33, and 24 × 10^{-3} mol g^{-1} min^{-1} (Table 3). Since no significant differences in yields are apparent, rehydration of 0.5 h is considered the optimum.

In the case of 2-propanol cyanoethylation over 3MgAl, an increased rehydration time had a more significant effect. As may be observed in Fig. 9, acrylonitrile conversions at 120 min reaction time are 74% and 58% over catalysts rehydrated for 1 and 0.5 h, respectively. Corresponding yields at 60 min are 63.4% and 48.2% (Table 3). It is worth noting that with methanol, the maximum conversion is reached very fast, in ~25 min. In contrast, with 2-propanol, conversion continually increases with time (Fig. 9). This observation further supports the hypothesis that there is a different rate-limiting step of the reaction mechanism (Scheme 1) for each of the studied alcohols.

Similarly, cyanoethylation of 2-propanol was carried out over catalysts with Mg/Al ratio of 2 and varying rehydration times. As observed in Fig. 10, conversion is slightly higher over 2MgAl-R1 than over 2MgAl-R0.5, while it is significantly lower over 2MgAl-R3. Therefore, basic strength diminishes when the catalyst is rehydrated for 3 h, due to the poisoning effect of excess water, as discussed previously (Section 3.1.3.3). Yields at 60 min are 65%, 69%, and 50% for 2MgAl-R05, 2MgAl-R1 and 2MgAl-R3. Initial reaction rates reveal a similar trend, increasing from 12 to 13 × 10^{-3} mol g^{-1} min^{-1} for catalysts rehydrated for 0.5 and 1 h, and then decreasing to 8 × 10^{-3} mol g^{-1} min^{-1} for catalyst rehydrated for 3 h.

On the other hand, increasing rehydration time up to 3 h on the less active catalysts, 3.5MgAl and 4MgAl, had a marked positive effect on conversion. As an example, Fig. 11 presents results of cyanoethylation of methanol over 3.5MgAl-R0.5 and 3.5MgAl-R3. On catalyst with 0.5 h rehydration, conversion continues to increase with time, reaching 92% after 85 min. In a shorter time, 50 min, 3.5MgAl-R3 has reached 90%, and at 90 min, conversion is nearly 99%. It is also interesting to notice that these two catalysts show an activation stage of about 5 min, during which time there is no catalytic activity. Likewise, among the catalysts with Mg/Al ratio of 4, the only one that displayed slight activity for cyanoethylation

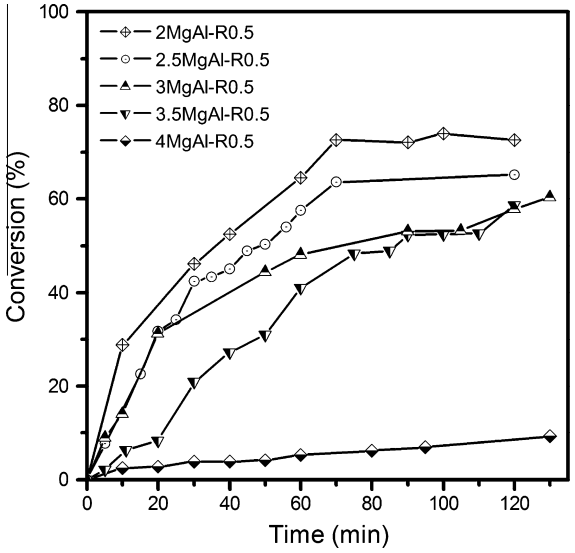

Fig. 8. Cyanoethylation of 2-propanol over catalysts with varying Mg/Al molar ratios and 0.5 h rehydration time.

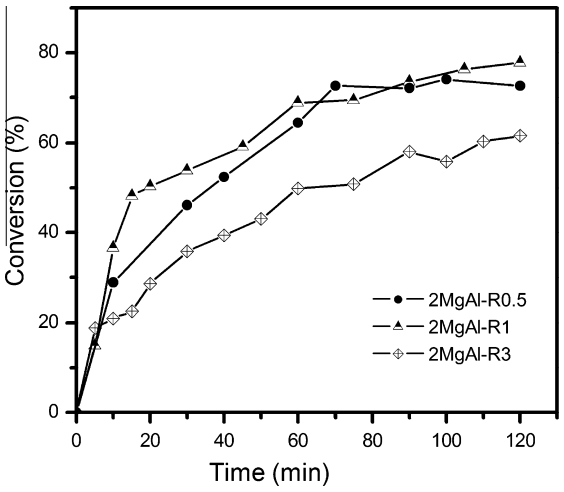

Fig. 10. Cyanoethylation of 2-propanol over catalyst 2MgAl with varying rehydration times.

of methanol was the one rehydrated for 3 h. Furthermore, the activation period for this catalyst was considerably longer, of ~30 min (Fig. 11).

Cyanoethylation activities displayed by the LDHs rehydrated under H_2O/N_2 flow at 80 °C are superior to many of the solids studied thus far, and the catalysts present several advantages. For instance, conversions above 80% are obtained for the cyanoethylation of 2-propanol over CaO and La_2O_3, but the catalysts are nearly inactive for the cyanoethylation of methanol [2]. Similar phenomena are observed with other basic solids, such as $Ba(OH)_2{\cdot}8H_2O$ and $Sr(OH)_2{\cdot}8H_2O$, which are highly active for cyanoethylation of ethanol and unreactive toward 2-propanol [2]. BaO shows conversions above 60% for methanol, ethanol and 2-propanol, but requires activation pretreatment at very high temperature (1000 °C) [2]. With rare-earth modified LDHs, for the cyanoethylation of ethanol, conversions of ~40% are obtained, with ~90% selectivity to β-ethoxypropionitrile [4]. Conversely, a MgAl LDH activated at room temperature was found to be highly active for the cyanoethylation of several alcohols [3]. Nonetheless, the activation procedure is too time-consuming for industrial applications, an obstacle that may be surmounted by following the procedure here presented.

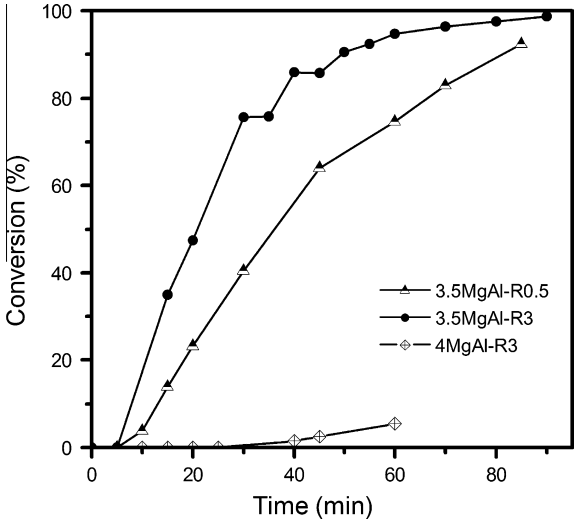

Fig. 11. Cyanoethylation of methanol over indicated catalysts.

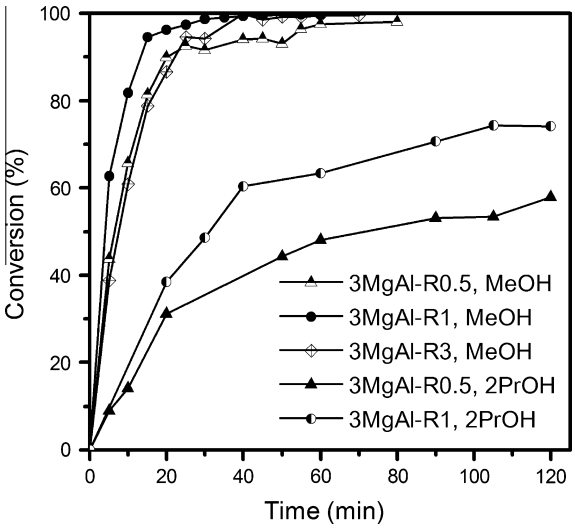

Fig. 9. Cyanoethylation of methanol or 2-propanol over catalyst 3MgAl with varying rehydration times.

4. Conclusions

MgAl LDHs with varying Mg/Al molar ratios were calcined and rehydrated to obtain highly active basic catalysts. Rehydration was carried out on the gas phase, using an H_2O/N_2 flow at 80 °C. In this way, the process is shortened from the average 12 h at room temperature to only 0.5 h. Solids thus obtained presented a regenerated layered structure, with OH^- groups acting as interlayer charge-balancing anions and as Brönsted basic sites. The strength of these sites was assessed by $CDCl_3$ adsorption followed by FTIR. It was found that basic strength decreases with increasing Mg/Al molar ratio. The catalysts were tested for the cyanoethylation of alcohols (methanol and 2-propanol), an industrially important reaction from which carboxylic acids and amines are obtained. Excellent conversions were obtained with 100% selectivity. A correlation between catalytic activities and basic strengths was proposed. It appears that for cyanoethylation of 2-propanol and

larger alcohols, particularly of branched alcohols, solids with very strong basic sites should be designed. Furthermore, the faster catalyst regeneration process presented here may facilitate industrial application of activated LDHs.

Acknowledgments

This work was financially supported by Instituto Mexicano del Petroleo and Universidad Autonoma Metropolitana. Authors thank PAPIIT-UNAM, Conacyt and SEP-PROMEP for grants IN107110, 60868 and UAM-PTC-104, respectively. J. P. thanks Conacyt for a Ph.D. scholarship. Alejandra Santana's technical support is gratefully acknowledged.

Appendix A. Supplementary material

Spectra taken prior and subsequent to $CDCl_3$ adsorption, and then during thermal decomposition, of all analyzed catalysts, may be found online as supplementary material. Supplementary data associated with this article can be found, in the online version, at doi:10.1016/j.jcat.2011.01.018.

References

[1] M.J. Astle, R.W. Etherington, Ind. Eng. Chem. 44 (1952) 2871.
[2] H. Kabashima, H. Hattori, Catal. Today 44 (1998) 277.
[3] P.S. Kumbhar, J. Sanchez-Valente, F. Figueras, Chem. Commun. (1998) 1091.
[4] E. Angelescu, O.D. Pavel, M. Che, R. Birjega, G. Constentin, Catal. Commun. 5 (2004) 647.
[5] R. Birjega, O.D. Pavel, G. Costentin, M. Che, E. Angelescu, Appl. Catal. A 288 (2005) 185.
[6] F. Cavani, F. Trifiro, A. Vaccari, Catal. Today 11 (1991) 173.
[7] V. Rives (Ed.), Layered Double Hydroxides: Present and Future, Nova Science Publishers, Inc., New York, 2001.
[8] X. Duan, D.G. Evans (Eds.), Layered Double Hydroxides, Struc. & Bonding, vol. 119, Springer-Verlag, Berlin Heidelberg, Germany, 2006.
[9] P.S. Kumbhar, J. Sanchez-Valente, J. Lopez, F. Figueras, Chem. Commun. (1998) 535.
[10] F. Figueras, Top. Catal. 29 (2004) 189.
[11] J.S. Valente, F. Tzompantzi, J. Prince, J.G.H. Cortez, R. Gomez, Appl. Catal. B 90 (2009) 330.
[12] K.K. Rao, M. Gravelle, J.S. Valente, F. Figueras, J. Catal. 173 (1998) 115.
[13] F. Prinetto, G. Ghiotti, R. Durand, D. Tichit, J. Phys. Chem. B 104 (2000) 11117.
[14] J.C.A.A. Roelofs, D.J. Lensveld, A.J. van Dillen, K.P. de Jong, J. Catal. 203 (2001) 184.
[15] M.J. Climent, A. Corma, S. Iborra, A. Velty, J. Catal. 221 (2004) 474.
[16] K. Ebitani, K. Motokura, K. Mori, T. Mizugaki, K. Kaneda, J. Org. Chem. 71 (2006) 5440.
[17] O.D. Pavel, R. Bîrjega, M. Che, G. Costentin, E. Angelescu, S. Şerban, Catal. Commun. 9 (2008) 1974.
[18] J.A. van Bokhoven, J.C.A.A. Roelofs, K.P. de Jong, D.C. Koningsberger, Chem. Eur. J. 7 (2001) 1258.
[19] T. Hibino, A. Tsunashima, Chem. Mater. 10 (1998) 4055.
[20] J.C.A.A. Roelofs, J.A. van Bokhoven, A.J. van Dillen, J.W. Geus, K.P. de Jong, Chem. Eur. J. 8 (2002) 5571.
[21] M. Bellotto, B. Rebours, O. Clause, J. Lynch, D. Bazin, E. Elkaim, J. Phys. Chem. 100 (1996) 8535.
[22] W. Yang, Y. Kim, P.K.T. Liu, M. Sahimi, T.T. Tsotsis, Chem. Eng. Sci. 57 (2002) 2945.
[23] E. Kanezaki, Sol. State Ionics 106 (1998) 279.
[24] F. Winter, X. Xia, B.P.C. Hereijgers, J.H. Bitter, A.J. van Dillen, M. Muhler, K.P. de Jong, J. Phys. Chem. B 110 (2006) 9211.
[25] R.J. Chimentão, S. Abelló, F. Medina, J. Llorca, J.E. Sueiras, Y. Cesteros, P. Salagre, J. Catal. 252 (2007) 249.
[26] F. Millange, R.I. Walton, D. O'Hare, J. Mater. Chem. 10 (2000) 1713.
[27] B. Rebours, J.B. d'Espinose de la Caillerie, O. Clause, J. Am. Chem. Soc. 116 (1994) 1707.
[28] N.S. Puttaswamy, P.V. Kamath, J. Mater. Chem. 7 (1997) 1941.
[29] T. Stanimirova, T. Hibino, V. Balek, J. Therm. Anal. Calorim. 84 (2006) 473.
[30] J.S. Valente, E. Lima, J.A. Toledo-Antonio, M.A. Cortes-Jacome, L. Lartundo-Rojas, R. Montiel, J. Prince, J. Phys. Chem. C 114 (2010) 2089.
[31] H. Pfeiffer, E. Lima, V. Lara, J.S. Valente, Langmuir 26 (2010) 4074.
[32] H. Pfeiffer, L. Martínez-dlCruz, E. Lima, J. Flores, M.A. Vera, J.S. Valente, J. Phys. Chem. C 114 (2010) 8485.
[33] S. Abelló, D. Vijaya-Shankar, J. Pérez-Ramírez, Appl. Catal. A 342 (2008) 119.
[34] J. Sanchez-Valente, E. Lopez-Salinas, M. Sanchez-Cantu, US Patent 7 807 128 B2, 2010, to Instituto Mexicano del Petróleo.
[35] J.S. Valente, M.S. Cantu, F. Figueras, Chem. Mater. 20 (2008) 1230.
[36] J.S. Valente, M. Sanchez-Cantu, E. Lima, F. Figueras, Chem. Mater. 21 (2009) 5809.
[37] R.D. Shannon, Acta Cryst. A32 (1976) 751.
[38] I. Pausch, H.H. Lohse, K. Schürmann, R. Allmann, Clays Clay Miner. 34 (1986) 507.
[39] J.S. Valente, J. Prince, A.M. Maubert, L. Lartundo-Rojas, P. del Angel, G. Ferrat, J.G. Hernandez, E. Lopez-Salinas, J. Phys. Chem. C 113 (2009) 5547.
[40] J.C. Lavalley, Catal. Today 27 (1996) 377.
[41] H. Knözinger, S. Huber, J. Chem. Soc. Faraday Trans. 94 (1998) 2047.
[42] E.A. Paukshtis, N.S. Kotsarenko, L.G. Karakchiev, React. Kinet. Catal. Lett. 12 (1979) 315.
[43] E.A. Paukshtis, E.N. Yurchenko, Russ. Chem. Rev. 52 (1983) 242.
[44] K. Nakamoto, Infrared and Raman Spectra of Inorganic and Coordination Compounds, fifth ed., John Wiley & Sons, New York, 1997.
[45] E. Lopez-Salinas, M. García-Sánchez, M.E. Llanos-Serrano, J. Navarrete-Bolaños, J. Phys. Chem. B 101 (1997) 5112.
[46] P. Kustrowski, D. Sułkowska, L. Chmielarz, R. Dziembaj, Appl. Catal. A 302 (2006) 317.